Experimental Study of a Switched Reluctance Motor Stator Tooth with Wet Slot and End Winding Cooling

Jasper Nonneman[a,b], Stephan Schlimpert[c], Ilya T'Jollyn[a,b] and Michel De Paepe[a,b]

[a] *Department of Electromechanical, Systems and Metal Engineering, Ghent University, Sint-Pietersnieuwstraat 41, 9000 Ghent, Belgium, Jasper.Nonneman@UGent.be CA, Ilya.TJollyn@UGent.be, Michel.DePaepe@UGent.be*
[b] *Flanders Make@UGent – Core lab EEDT-MP, Gent, Belgium*
[c] *Flanders Make, Core Lab MotionS, Gaston Geenslaan 8, 3001, Leuven, Belgium, Stephan.Schlimpert@FlandersMake.be*

Abstract:

This paper presents an experimental study of direct coil cooling applied to a stator tooth of a switched reluctance motor where a direct contact is realized between the winding and fluid. Experiments were performed with a setup consisting of one tooth of a SRM without rotor, but including stator iron and one preformed winding. Three configurations of the cooling method were investigated: slot cooling, end winding cooling and a combination of the two by pumping an Automatic Transmission Fluid (ATF) over the designated sides of the winding. The setup is equipped with 17 thermocouples integrated within the components to determine the temperatures. Three inlet temperatures (21, 33 and 44°C) and four flow rates (1.5, 2, 3.5 and 5 l/min) of the coolant were tested at four different heat losses in the winding (10, 30, 50 and 70W). The results show that the maximum temperature is always located in the centre of the winding and is the lowest for the combined cooling (73.0°C), followed by the slot cooling (79.7°C) and then by the end winding cooling (91.6°C) for the lowest ATF inlet temperature and the highest heat losses and flow rate. With a determined current density in the range 13.8A/mm² to 19.5 A/mm², all three direct coil cooling methods show a great potential in increasing the power density of electric motors.

Keywords:

Direct coil cooling, Electric motor cooling, End winding cooling, Experimental study, Switched Reluctance Motor, Wet slot cooling.

1. Introduction

Electrical alternatives to combustion engines in the transport sector become more and more popular. These electrified drivetrains, consisting of batteries, power electronics and an electric motor, experience the trend to get more power dense. As a result, the cooling limit of the conventional cooling methods such as a liquid jacket, starts to be reached and excessive temperatures are attained within the components of the drivetrain [1].

The most commonly used electric motor in these drivetrains is a Permanent Magnet Synchronous Motor (PMSM), but these make use of rare earth materials for the permanent magnets. A successfully proven alternative is a Switched Reluctance Motor (SRM), which does not use these rare earth materials and can attain similar rotational speeds, torque and efficiency [2]. A SRM consists of an iron laminated stator with copper windings and a laminated rotor. The temperature in the winding is mostly the bottleneck to go to higher power densities and peak powers in this type of motor because of the long thermal path from winding to jacket, the low thermal conductivity of the winding in radial and tangential direction [3] and the significant Joule heating in the wires. As a result, more effective cooling methods are needed for the windings specifically to increase the power density further. One

1

of the possibilities is to cool the winding more directly within the slot or at the end windings with a dielectric fluid [1, 4].

Popescu et al [5] show the possibility to cool the stator windings with forced liquid (Paratherm LR) through the slot and to cool the end windings with oil from the transmission of the motor. Márquez-Fernández et al [6] experimentally investigated the direct cooling of the windings of a Yokeless And Segmented Armature (YASA) axial flux switched reluctance machine. A gap was left open between the coil and stator iron so that fluid can circulate between the two components. Camilleri et al used a similar cooling configuration and developed a method to optimize the flow geometry with the aim of improving the temperature distribution and reducing the hot spot temperature. Liu et al. [7] studied the direct coil cooling in the stator slots of a switched reluctance motor with oil and the addition of baffles to improve the heat transfer. Wohlers et al [8] investigated two different coil designs for direct liquid cooling to allow a better contact between fluid and winding. This was done by systematically removing winding material such that several cooling channels remain within the slot. Nonneman et al [9] did a simulation based comparison of jacket cooling and dry and wet direct coil cooling.

The previously mentioned studies show the great potential of both slot cooling and end winding cooling by forced convection. Within this paper, the performance of both methods is experimentally evaluated on a stator tooth of a radial switched reluctance machine, together with the combination of the two methods. The performance of the methods is compared, based on the maximum winding and stator iron temperatures, which should be as low as possible. Only one stator tooth was used for the experiments due to symmetry of the motor and to limit the complexity of the experimental setup (no rotating machine). The experimental setup used for these measurements was designed and built within the framework of the ICON Hipercool project.

Firstly, the motor geometry and the configuration of the direct coil cooling methods are described. Then the used experimental setup and test sections are shown and the measurement procedure is described. Finally, the measurement results are discussed and the different methods are compared to each other and to other electric motor cooling methods.

2. Geometry description

2.1. Machine overview

The motor type studied within this paper is a radial switched reluctance motor as shown in Fig. 1. It consists of a laminated stator that generates a magnetic field using power delivered to the stator coils. The rotor only consists of iron laminations and tends to go to a minimum state of reluctance. The use of preformed concentrated stator windings (which have a high filling factor) leaves a triangular space in the slot between the adjacent windings and stator yoke due to the conical shape of the slot, which can be used as a channel for direct coil cooling in the slot. Filling the slot completely with wires is also possible but this typically results in a lower filling factor. In that case, some space should be sacrificed for cooling. Within this paper, preformed stator windings will be studied which leave an open triangular space where oil can be pumped through to cool the windings at the slot. The motor parameters of the used motor geometry are shown in Table 1.
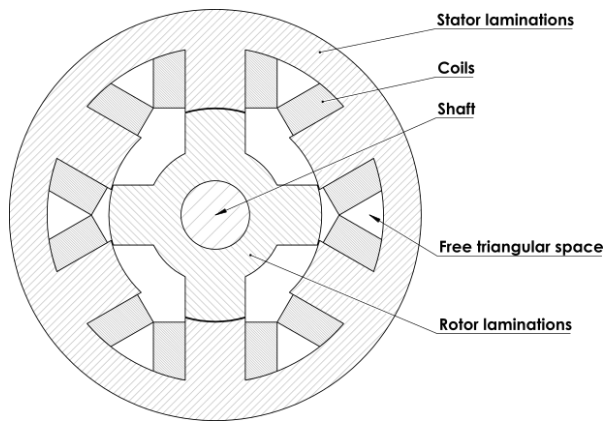
2

Fig. 1. Typical sectional view of a 6/4-SRM.

Table 1. Motor parameters of the studied geometry [10]

Parameter	Value
Stator/rotor poles	6/4
Axial active length	80 mm
Shaft diameter	20 mm
Rotor outer diameter	62 mm
Stator outer diameter	120 mm
Airgap thickness	0.25 mm
Yoke thickness	11 mm
Pole width	17.5 mm
Rated speed	3000 rpm
Rated power	3 kW

2.2. Studied cooling methods and configuration

The two cooling methods that are studied within this paper cool the winding at a different geometrical location. The direct winding cooling within the slot uses the free triangular space between the coils to cool the lateral side of the windings, as indicated in Fig. 2 (left). In this configuration, the fluid is also in contact with the stator iron and therefore the fluid cools this surface. In case of end winding cooling, the fluid is only in contact with the surfaces of the winding at the end space, more specifically with every outer surface except the end winding side facing the shaft as shown in Fig. 2 (centre). The surface facing the shaft side is not cooled in this study due to practical considerations: sealing of the fluid from the airgap, rotor and end space. Further, also a combination of these two methods is studied as shown in Fig. 2 (right).
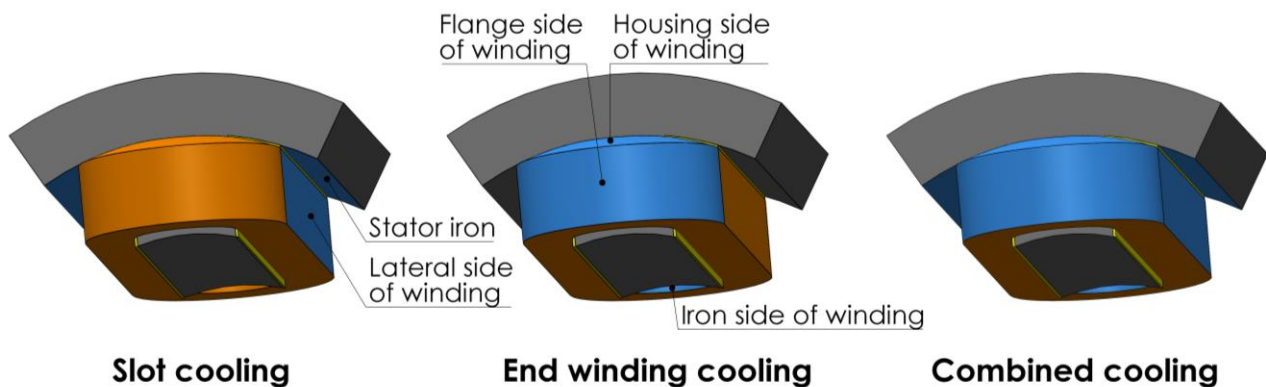

Fig. 2. Cooling method configurations and cooled surfaces (in blue): slot cooling (left), end winding cooling (centre) and a combination (right)

3. Experimental setup

3.1. Overview

A new experimental setup was designed based on a water-glycol cooling circuit that was built earlier in the project [11]. The design is similar, except that an Automatic Transmission Fluid (ATF) is used instead of a mixture of water-glycol, to allow direct contact between the fluid and the windings without causing a short circuit. More specifically the used ATF is DEXRON-VI ATF, which is a passenger car lube. The cooling circuit is not specifically designed for the stator tooth only, but also

3

different drive train components (power electronics; motor tooth; DC-DC charger; etc.) can be experimentally investigated in an automatic, fast, efficient and accurate manner due to a plug and play design with respect to the test section. The ATF is stored within a reservoir and circulated through the fluid conditioning circuit and test section by a gear pump as shown on Fig. 3. After cooling the test section, the ATF flows through a chiller tank to bring it to the desired fluid temperature. Heat losses from the fluid to the ambient are minimized by maintaining the ambient temperature as close as possible to the fluid temperature with an HVAC system in the lab.
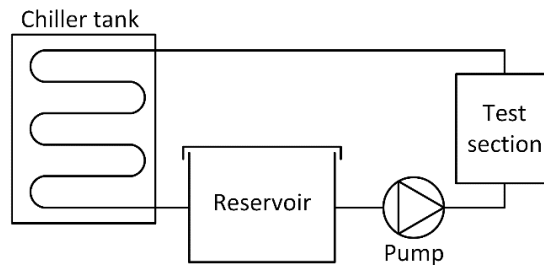

Fig. 3. Fluid conditioning circuit and test section.

3.2. Test section

The same casing and assembly of the stator tooth of a SRM without rotor - consisting of stator iron, one impregnated winding and Nomex liner between winding and stator pole/yoke - is used to investigate the different cooling methods. The only difference between the cooling configurations is the type of end space inserts that was used to be able to cool the desired winding surfaces and to shield those surfaces that should not be cooled. The two types of test sections are shown in Fig. 4 for slot cooling (left) and end winding cooling or a combination (right). The hydraulic connection is different for each cooling method and is shown in Fig. 5. The practical implementation of the hydraulic connection is shown in Fig. 5 for the slot cooling (top right) and end winding cooling (bottom right). In all cases, the channels are connected to the ATF conditioning circuit and the flow is distributed in a parallel configuration over the different channels. The casing and inserts are manufactured by 3D printing out of low conductive material (polyamide) to be able to keep the components together, constrain the ATF and limit heat losses from the test section to the environment.
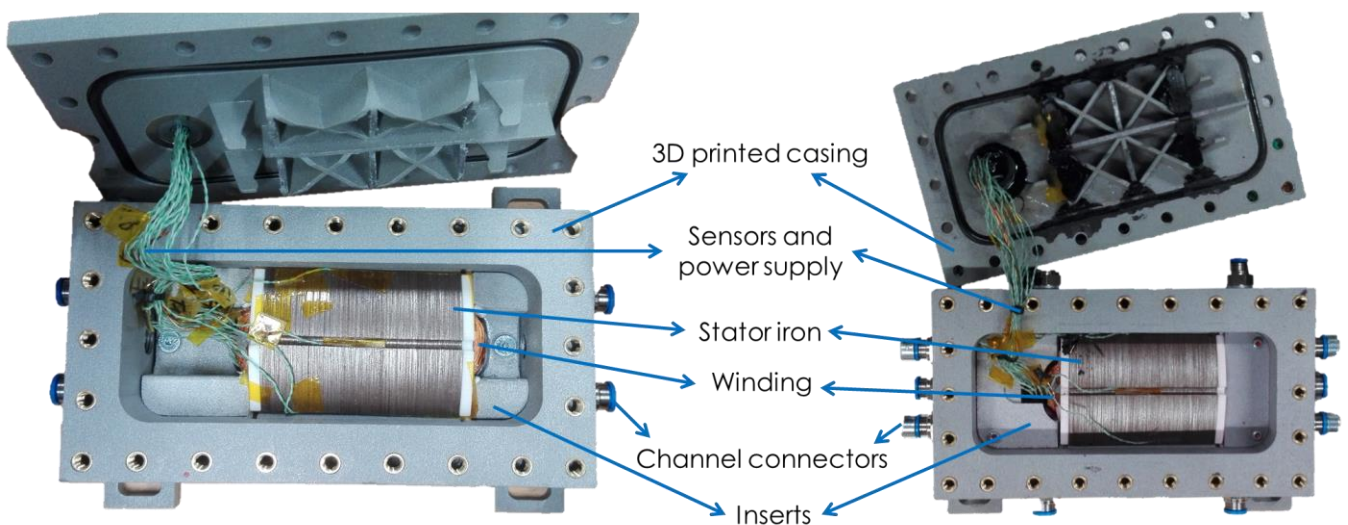

Fig. 4. Stator tooth test section for slot cooling (left) and end winding cooling or a combination (right)
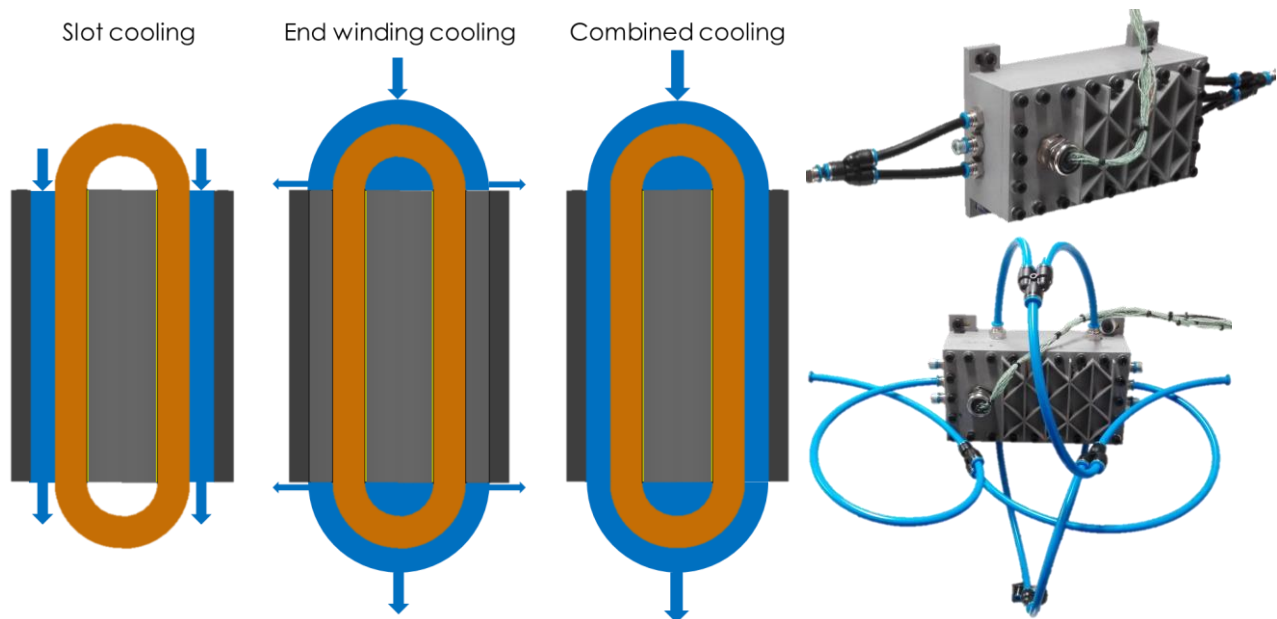
Fig. 5. Stator tooth bottom view with the hydraulic connection of the different cooling configurations (left) and practical implementation of slot cooling (top right) and end winding cooling (bottom right).

3.3. Sensors

Several sensors are included within the setup to determine the thermal performance of the cooling methods. Two PT100 temperature sensors measure the fluid temperature at the inlet and outlet of the test section. An ultrasonic flow meter measures the volumetric flow rate through the setup. The electrical DC current supplied to the winding to dissipate the necessary heat is determined by measuring the voltage and current. The uncertainty of the electric power measurement can be determined based on the uncertainty on the voltage and current measurement.

Seventeen K-type thermocouples are distributed within the stator tooth to map the temperature distribution and temperature drops over the interfaces as complete as possible. Fig. 6 shows the location of the temperature sensors. The fluid enters the test section at the side of slice A in case of slot cooling and combined cooling. Sensors 1-8 measure the winding temperature in the active and end winding region. Sensors 9-17 measure the iron temperature at different locations in the active part. An overview of the range and uncertainty of the sensors within the setup is shown in Table 2.

Table 2. Range and uncertainty of the sensors.

Sensor	Range	Uncertainty
PT100	-50…120°C	±0.15°C
K-type thermocouple	-50…250°C	±1°C
Ultrasonic flow meter	0.3…21 l/min	±1% or ±0.014 l/min
Current	0…75A	±1%
Voltage	0…200V	±1%

Due to the difficulty of positioning the thermocouples accurately, the actual location can slightly deviate from the intended location. The hot junction of the thermocouples located at the interface of two components or at the heat transfer surface with the fluid, can be in a better thermal contact with one of the two components/fluid. Thereby, it can measure only one of the two temperatures, or measure an average of the two temperatures. As a result, it is expected that the uncertainty on the temperature measurement indicated in Table 2 is rather optimistic.
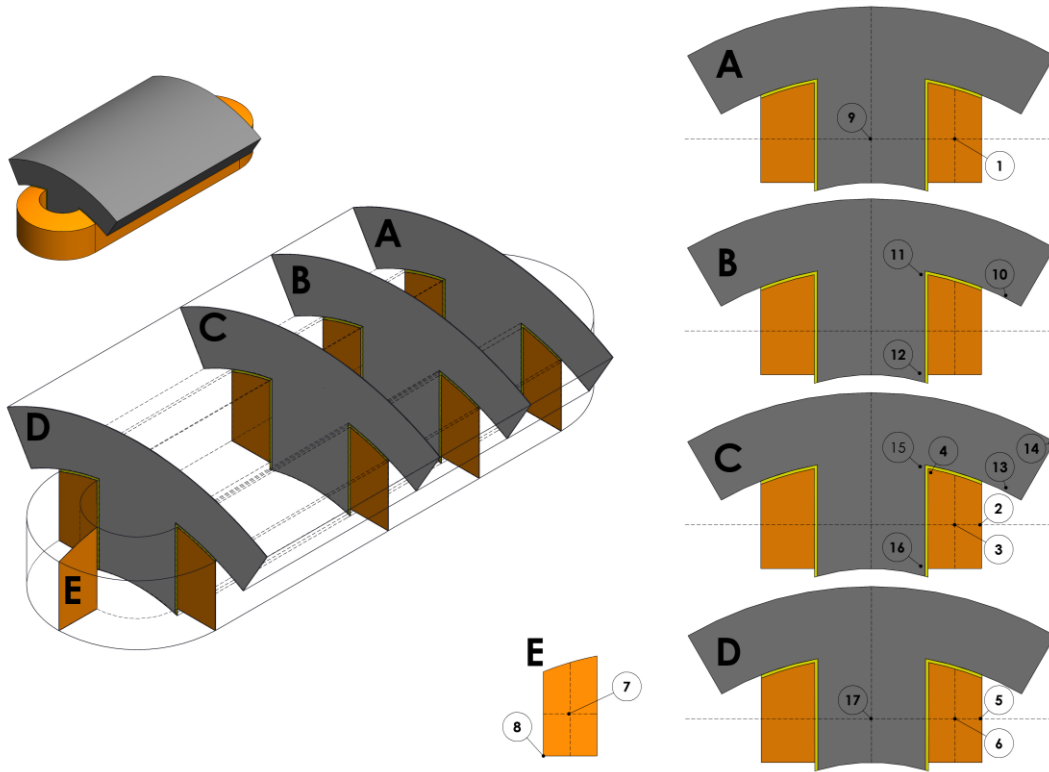
5

Fig. 6. Thermocouple locations in the stator tooth setup with the slices A, B, C and D in the active part, and slice E in the end winding part.

3.4. Measurement plan and procedure

Measurements were performed for three fluid inlet temperatures (21°C, 33°C and 44°C) which are common in electric vehicles, except for end winding cooling where the 33°C inlet temperature was not measured. To study the influence of the convective heat transfer coefficient, three different flow rates of the coolant were investigated (2, 3.5 and 5 l/min) at four different heat losses in the winding (10, 30, 50 and 70 W). In case of end winding cooling, one additional and lower flow rate was investigated: 1.5 l/min.

The following semi-automated procedure was followed:
- Manually configure a certain cooling configuration.
- Set a certain fluid inlet temperature along with the corresponding lab temperature (T_{amb} = 20°C for T_{in} = 21°C; T_{amb} = 28°C for T_{in} = 33 and 44°C).
- Run for 4h at the highest flow rate without heat losses in the winding to get the chiller tank and reservoir to a stable temperature.
- Start the test in order of decreasing flow rate and for every flow rate, an increasing heating power.
- Measure one stable setpoint for a period of 10 min to get steady state values and limit the measurement noise.

Between every other heat loss setpoint there was a stabilization time of 30 min, which was sufficient due to the low thermal inertia of the stator tooth and small steps in the setpoints. Between different setpoints of the flow rate, a stabilization time of 10 min was used. One complete test procedure for one cooling configuration and fluid temperature (~13h) is fully automated with the above mentioned stabilization times such that no deviations between the different fluid temperature setpoints are expected.

4. Measurement results and discussion

The measurement results will be analysed based on the maximum temperatures measured in the different regions (end winding region, active region and surfaces at the end of the active region) and components (winding and iron) of the motor. The maximum temperature in a certain component region is always measured by the same sensor for a specific cooling method. Table 3 shows these fixed temperature sensors for each region and cooling method. The sensor measuring the overall maximum temperature is indicated in bold-underlined. The sensors measuring lower temperatures are further not analysed within this paper, but will be used for validation purposes of a thermal model in a next publication.

These sensors specifically measure the maximum temperatures because of the following reason:
- Sensor 7 is the only sensor that is located at the centre of the end winding and obviously measures the maximum temperature here (hot spot).
- Sensors 6 and 17 are located the furthest from the inlet (slot and combined cooling) resulting in a higher ATF temperature at this axial location and a lower convection coefficient compared to the inlet (developing flow). In case of end winding cooling, sensor 1 measures the maximum temperature but the difference with sensor 6 is small (sensors measure similar temperatures due to symmetry).
- Sensors 3 and 16 are located at the middle slice of the motor, at the locations the furthest away from the fluid.

Table 3. Sensors measuring the maximum temperature within specific regions and components.

Component	Region	*Slot cooling*	*End winding cooling*	*Combined*
Winding	End winding region	*<u>7</u>*	*7*	*<u>7</u>*
Winding	Surfaces at the end of active region	*6*	*6*	*1*
Winding	Active region	*3*	*<u>3</u>*	*3*
Iron	Surfaces facing end space	*17*	*17*	*17*
Iron	Active region	*16*	*16*	*16*

At first, the influence of the heat losses and fluid inlet temperature on the maximum temperature will be checked. To be able to compare the measurement results at different inlet temperatures and heat losses, a maximum thermal resistance R_{max} from fluid inlet temperature to the maximum temperature T_{max} is determined, based on the total dissipated heat in the winding P_{cu} with Eq. (1):

$$R_{max} = \frac{T_{max} - T_{in}}{P_{cu}} \qquad (1)$$

Taking into account the propagation of errors, the uncertainty on this maximum thermal resistance δR_{max} is determined with Eq. (2):

$$\delta R_{max} = \frac{1}{VI} \sqrt{\delta T_{max}^2 + \delta T_{in}^2 + (T_{max} - T_{in})^2 \left(\frac{\delta V^2}{V^2} + \frac{\delta I^2}{I^2}\right)} \qquad (2)$$

With δT_{max} and δT_{in} respectively the uncertainty on the thermocouple and PT100 measurement, V and δV respectively the value and uncertainty of the voltage measurement and I and δI respectively the value and uncertainty of the current measurement.

Fig. 7. (left) shows the effect of the winding heat loss on the maximum thermal resistance for the highest flow rate (5 l/min) and lowest inlet temperature (21°C). The three coloured lines indicate the different cooling methods, which are respectively sensor 7, 3 and 7 for slot, end winding and

combined cooling. The figure shows that the uncertainty of the thermal resistance is relatively big for the smallest heat loss, while it decreases with increasing heat loss. Considering this uncertainty, it can be concluded that the influence of the heat loss on the thermal resistance is rather small and within the measurement uncertainty for the three cooling methods. Fig. 7 (right) shows the effect of the oil inlet temperature on the maximum thermal resistance for the highest flow rate (5 l/min) and highest heating power (70 W). The thermal resistance slightly increases with an increasing inlet temperature for slot cooling, while it decreases for end winding cooling and is constant for combined cooling. No conclusive explanation can be given for this result, but it can be caused by diverging changes in flow patterns for the three methods due to a change in fluid properties with temperature (mostly viscosity μ, which is $\mu_{ATF,21°C} = 0.0657$ Pa-s and $\mu_{ATF,44°C} = 0.0254$ Pa-s).

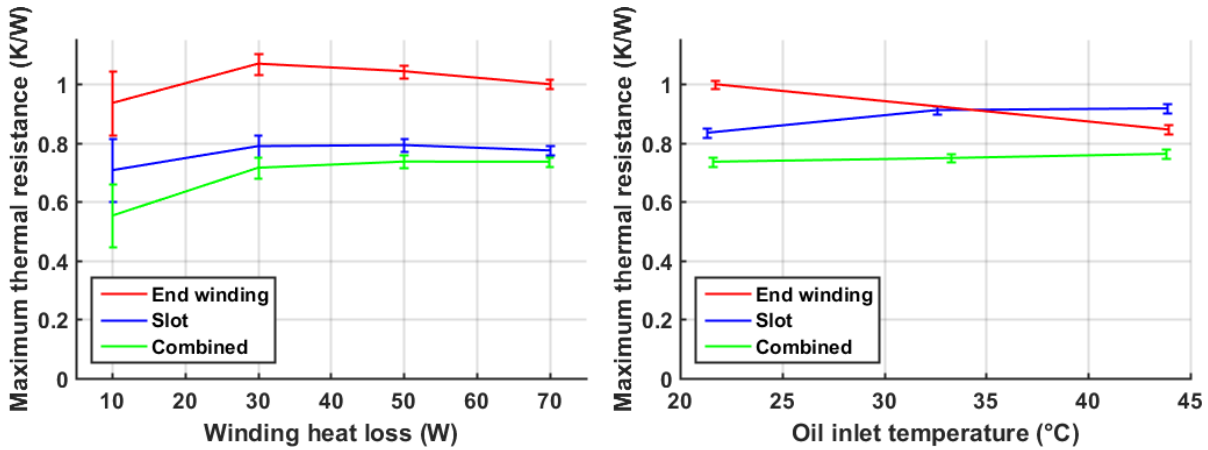*Fig. 7. Influence of winding heat losses at T_{in} =21°C (left) and oil inlet temperature at P_{cu} = 70W (right) on the maximum thermal resistance for the highest flow rate (5 l/min).*

Fig. 8 shows the maximum temperatures measured within the winding (left) and iron (right) by the sensors from Table 3 for the highest heat losses (70 W) and lowest inlet temperature (21 °C). Several conclusions can be drawn from these figures. Firstly, it can be seen that the thermal resistance decreases with increasing flow rate, which is the obvious effect of a higher heat transfer coefficient between winding and fluid and a lower outlet temperature at higher flow rates. When increasing the flow rate from 2 l/min to 5 l/min, the maximum temperature decreases with about 6 to 10°C for the different configurations. In case of slot and combined cooling, the winding temperature measured by sensor 7 is around 5°C higher than the temperature measured by sensor 3 and 6, while for end winding cooling the difference is within the measurement uncertainty. The reason is that the hot spot is located within the end winding for slot and combined cooling, while for end winding cooling the temperature in the centre of the winding is relatively uniform. Looking at the difference in iron temperature measured by sensors 16 and 17, the difference is similar for the different methods and closely within the measurement uncertainty.

When comparing the different methods with each other at the same flow rate, the maximum temperature decreases from end winding cooling to slot cooling to the combination of the two methods. At the highest flow rate, the maximum winding temperature is around 12°C lower for slot cooling than end winding cooling and 19°C lower for combined cooling than end winding cooling. The maximum iron temperature is around 19°C lower for slot cooling than for end winding cooling and 23°C lower for combined cooling than for end winding cooling. The higher difference for the iron temperature is caused by the fact that the iron is directly cooled in case of slot and combined cooling, while for end winding cooling the stator iron is only indirectly cooled through the winding itself.
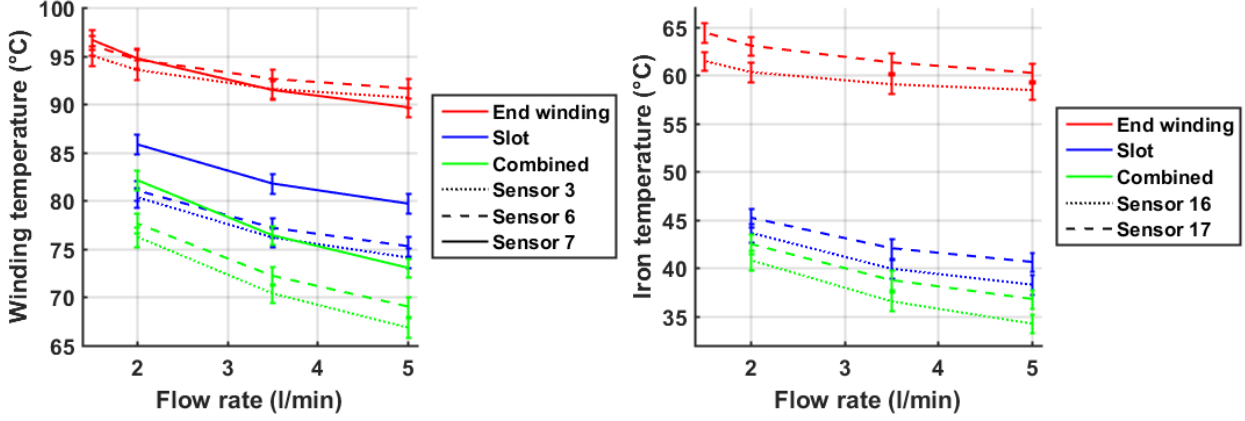
8

Fig. 8. Effect of the flow rate on maximum winding (left) and iron (right) temperature for the different cooling methods at the highest heat losses (70W) and lowest inlet temperature (21°C). The elements in the legend should be combined to obtain the labels of the lines.

To compare the cooling performance of the methods studied within this paper, an estimation of the maximal possible current density is determined for each cooling method and inlet temperature, based on the losses in the windings only. This maximal possible current density is reached when the winding hot spot temperature $T_{max\,F/H}$ equals 155°C for F-class windings and 180°C for H-class windings [12]. The estimation of the maximum current densities J_{max} is shown in Table 4 and is based on an extrapolation of the maximum thermal resistances R_{max} at the highest flow rate in Fig. 7 (right) and Eq. (3):

$$J_{max} = \frac{I_{meas}}{d_w^2 \pi/4} \sqrt{\frac{T_{max\,F/H} - T_{in}}{R_{max} P_{cu,meas}}} \qquad (3)$$

With d_w = 0.71mm the wire diameter of the used winding and $P_{cu,meas}$ and I_{meas} respectively the measured losses and measured current at the maximum thermal resistance.

Table 4. Estimated maximum current densities based on measurement results for class F and class H windings (unless otherwise specified, units are in A/mm²).

Inlet temperature	Slot cooling	End winding cooling	Combined
21°C	(F) 16.6 (H) 18.1	(F) 14.6 (H) 15.9	(F) 17.8 (H) 19.5
33°C	(F) 14.9 (H) 16.3	-	(F) 16.6 (H) 18.3
44°C	(F) 13.8 (H) 15.3	(F) 14.3 (H) 15.9	(F) 15.5 (H) 17.2

A comparison of the calculated values of the current densities (Table 4) with typical values for different motor cooling methods [4, 12], shows that they are at the maximum values that can be obtained with indirect forced liquid cooling (7-10 A/mm²[12] and 7-20A/mm² [4]) and are within the expected ranges for direct forced liquid cooling (10-30 A/mm²). It can be concluded that the three cooling methods have a great potential to replace jacket cooling when it has reached its maximum cooling limit.

Conclusion

Experiments have been performed to compare and investigate the thermal performance of several direct coil cooling methods for electric machines, where a direct contact between an ATF and the windings is realized. The test section consist of a SRM stator tooth equipped with 17 temperature sensors where a direct contact between an ATF and the windings is realized in three ways: at the slot, at the end windings and a combination of the two. In these experiments, the ATF inlet temperature, flow rate and heat losses in the windings are varied and the effect on the maximum temperature in the components is investigated based on the maximum thermal resistance.

The results show that the maximum temperature is always measured in the windings and the exact location is dependent on the cooling method: in the centre of the end winding for slot and combined cooling, and in the centre of the winding at the central axial slice for end winding cooling. The heat losses have a minor effect on the maximum thermal resistance, while the effect of the inlet temperature differs for each cooling method most presumably caused by different flow patterns due to a change in the viscosity of the ATF. The effect of an increasing flow is a reduction in the maximum winding temperature by about 6 to 10°C due to a higher heat transfer coefficient and a lower ATF outlet temperature.

Of the three configurations the combined cooling performs the best (T_{max} = 73.0°C), followed by the slot cooling (T_{max} = 79.7°C) and the end winding cooling (T_{max} = 91.6°C) for the lowest ATF inlet temperature and the highest heat losses and flow rate. The maximum possible current densities, determined from an extrapolation of the measurement results, are in the range 13.8A/mm² to 19.5 A/mm². A comparison with typical values for different motor cooling methods shows that the three configurations are a possible alternative for a typical jacket cooling when the latter has reached its cooling limits.

Acknowledgments

Nomenclature

d_w wire diameter, m
I current, A
J current density, A/mm²
P heat losses, W
R thermal resistance, K/W
T temperature, °C
V voltage, V

Greek symbols

δ uncertainty

Subscripts and superscripts

amb   ambient
ATF   Automatic Transmission Fluid
in   inlet
max   maximum
meas   measured

References

[1] Madonna V, Giangrande P, Walker A, Galea M, editors. On the effects of advanced end-winding cooling on the design and performance of electrical machines. 2018 XIII International Conference on Electrical Machines (ICEM); 2018: IEEE.

[2] Haghbin S, Rabiei A, Grunditz E, editors. Switched reluctance motor in electric or hybrid vehicle applications: A status review. 2013 IEEE 8th Conference on Industrial Electronics and Applications (ICIEA); 2013: IEEE.

[3] Siesing L, Reinap A, Andersson M, editors. Thermal properties on high fill factor electrical windings: Infiltrated vs non infiltrated. 2014 International Conference on Electrical Machines (ICEM); 2014: IEEE.

[4] Gai Y, Kimiabeigi M, Chong YC, Widmer JD, Deng X, Popescu M, et al. Cooling of automotive traction motors: schemes, examples, and computation methods. IEEE Transactions on Industrial Electronics. 2018;66(3):1681-92.

[5] Popescu M, Staton DA, Boglietti A, Cavagnino A, Hawkins D, Goss J. Modern heat extraction systems for power traction machines—A review. IEEE Transactions on Industry Applications. 2016;52(3):2167-75.

[6] Márquez-Fernández F, Potgieter J, Fraser A, McCulloch M. Thermal management in a high speed switched reluctance machine for traction applications. 2016.

[7] Liu Z, Winter T, Schier M, editors. Comparison of Thermal Performance between Direct Coil Cooling and Water Jacket Cooling for Electric Traction Motor based on Lumped Parameter Thermal Network and Experimentation. Electric Vehicle Symposium EVS28; 2015.

[8] Wohlers C, Juris P, Kabelac S, Ponick B. Design and direct liquid cooling of tooth-coil windings. Electrical Engineering. 2018;100(4):2299-308.

[9] Nonneman J, Clarie N, T'Jollyn I, Schlimpert S, Sergeant P, De Paepe M, editors. Advanced lumped parameter model for switched reluctance motors with high performance cooling. International Heat Transfer Conference; 2018.

[10] Ibrahim MNF, Sergeant P. Prediction of Eddy Current Losses in Cooling Tubes of Direct Cooled Windings in Electric Machines. Mathematics. 2019;7(11):1096.

[11] Nonneman J, Schlimpert S, T'Jollyn I, Sergeant P, De Paepe M, editors. Experimental Investigation of Direct Contact Baseplate Cooling for Electric Vehicle Power Electronics. 2019 18th IEEE Intersociety Conference on Thermal and Thermomechanical Phenomena in Electronic Systems (ITherm); 2019: IEEE.

[12] Polikarpova M. Liquid cooling solutions for rotating permanent magnet synchronous machines. 2014.